Eur. Phys. J. B **76**, 147–156 (2010)
DOI: 10.1140/epjb/e2010-00179-1

THE EUROPEAN PHYSICAL JOURNAL B

Regular Article

Network evolution based on minority game with herding behavior

B.A. Mello[1,a], V.M.C.S. Souza[2], D.O. Cajueiro[3,4], and R.F.S. Andrade[2,4]

[1] Instituto de Física – Universidade de Brasília, 70910-900 DF, Brazil
[2] Instituto de Física – Universidade Federal da Bahia, Salvador, 40210-340 BA, Brazil
[3] Departamento de Economia – Universidade de Brasília, 70910-900 DF, Brazil
[4] Instituto Nacional de Ciência e Tecnologia de Sistemas Complexos, Brazil

Received 31 August 2009 / Received in final form 29 March 2010
Published online 17 June 2010 –

Abstract. The minority game (MG) is used as a source of information to design complex networks where the nodes represent the playing agents. Differently from classical MG consisting of independent agents, the current model rules that connections between nodes are dynamically inserted or removed from the network according to the most recent game outputs. This way, preferential attachment based on the concept of social distance is controlled by the agents wealth. The time evolution of the network topology, quantitatively measured by usual parameters, is characterized by a transient phase followed by a steady state, where the network properties remain constant. Changes in the local landscapes around individual nodes depend on the parameters used to control network links. If agents are allowed to access the strategies of their network neighbors, a feedback effect on the network structure and game outputs is observed. Such effect, known as herding behavior, considerably changes the dependence of volatility σ on memory size: it is shown that the absolute value of σ as well as the corresponding value of memory size depend both on the network topology and on the way along which the agents make their playing decisions in each game round.

1 Introduction

In recent years, the study of dynamics and collective behavior of a population of agents competing for limited resources emerged as an active research area in complex systems [1,2]. A very simple such model that is able of producing a large amount of non trivial results is the so-called Minority Game (MG) [3], introduced as a simplification of Arthur's El Farol Bar [4] attendance problem. Any MG agent, in a population of size N, has to choose between two opposing actions, say $a = \pm 1$ based on a previously provided strategy. Since the resources are limited, the objective of each agent is to choose the winning side, i.e., the one shared by the minority of the population.

The standard MG has been intensively studied, and several revisions of its major properties are now available [2,5,6]. One of its most surprising properties [7] is summarized by plotting the ratio σ^2/N as a function of $\alpha = 2^M/N$, where the volatility of the attendance size σ is a measure of global efficiency of the system and M is the history remembrance of the agents about the previous game turns. The results indicate that: (i) for small values of α, the agents would perform worse than if they had taken purely random decisions. (ii) For large values of α, the agents' performance approaches the random decision. (iii) There is a critical value of $\alpha = \alpha_c$ where the resources of the game are used in the best possible way. At α_c, the ratio σ^2/N assumes its minimal value, suggesting a phase transition from the so-called low-M to the high-M phase. The low-M phase is characterized by a decrease in σ^2/N as α increases, while in the high-M phase such behavior is reversed. Excluding the trivial case where each agent has only one strategy, changing the number of strategies available for each agent does not qualitatively change MG outputs.

One interesting extension of MG considers that agents are allowed to access local information [8–18]. In a previous work [19], one of us analyzed a MG version where the local information exchange proceeds by the imitation of the best informed neighbor of any agent. One constraint of the quoted analysis [19] is that the agent's neighborhood had been provided by a static complex network before the game started, whereby four proxies for social networks [20–22] were considered: (1) regular networks; (2) random networks [23]; (3) small world networks [24,25]; and (4) a scale-free networks [26].

It is worth mentioning that this paper is related to several attempts that have tried to study social dynamics and the collective phenomena that emerge from the interaction among individuals [27,28]. In particular, those that have tried to model the flow of information through networks such as [29–32] and herding behavior [33,34].

The purpose of this work is to consider the situation where the networks evolve with time, based on the concept of social distance attachment [35]. To this purpose, pairs

[a] e-mail: bernardo@fis.unb.br

of MG players are allowed to establish links according to a decreasing function of a social distance, namely, the difference of their wealths accumulated in the previous turns of the game. This assumption quantifies, in a mathematical way, the idea of degree of closeness or acceptance of an individual in a group. The adopted procedure has two main consequences. The first one is to generate a network, independently of the fact that it can be used to influence the MG outcomes. In a second moment, we can use the obtained network to allow for interaction between agents, in such a way that they may use the strategies of their network neighbors to make the game options. This choice also introduces a feedback mechanism that can alter the evolution of the network itself.

Our proposal takes into account some previously discussed models and effects in social network evolution. In fact, several papers have assumed the hypothesis that the connecting probability between two nodes depend on the distance between them. For instance, in [36,37], the network links are introduced between similar nodes, where similarity is measured by the metric distance based on a dynamical process taking place on the network. In [38], the formation of links between two agents depends on a proximity measure, which is given by the number of mutual friends of these agents. The idea of distance has also been used in the spatial sense [39–41]. In that case, the agents are distributed in a geographical space, and the formation of an edge between two agents depends on the spatial distance between them. In [42], one may also find an empirical evidence of these types of networks.

This paper is organized as follows. In Section 2, a brief review of the standard MG and its extended version, with fixed local information exchange, is presented. Section 3 provides the explicit discussion of the model investigated herein, including both the algorithm used to build the agents' neighborhood as well as some analytical estimates.

A characterization of the topological properties of the obtained networks is presented in Section 4, which is divided in the following subsections: 4.1 - MG-Networks: the MG evolves as if the network did not exist. The network links are broken or established depending on the agents wealth. 4.2 - Feedback MG-networks: the agents communicate to each other through the network and the network evolves as previously described. 4.3 - ER-network and other measures: after an initial evolution as in the previous case, the network is frozen and the agents keep communicating through a fixed network.

Section 5 discusses how the network structure influences MG outcomes. We indicate that smaller values of volatility than those obtained by standard MG can be obtained within the proposed model. Finally, Section 6 closes the work with our concluding remarks.

2 MG basics and interaction mechanism

As anticipated in the Introduction, the MG rules are such that, at any given discrete instant of time, all playing agents choose either $a = 1$ or $a = -1$. This mimics, for instance, the decision of either buying or selling an asset in a financial market. The main feature of the game is the fact that each agent does not know other agents' decision. Thus, he has little information on how to choose the minority side. The agent decides on his next action based only on global information, which consists of the sequence of the last M outcomes of the game, where M also denotes the size of the agents' memory. There is no best solution for the problem, i.e., no agent knows the best strategy, defined as a set of prescriptions about which action should be taken, given the observed series of M last outcomes. Since there are only two possible choices, the number of possible outcomes is 2^M, what leads to a maximum of 2^{2^M} strategies. In [3] each agent has a fixed number of strategies that do not change over time. Since agents have different beliefs, the strategies differ from agent to agent. At every turn of the game, the agents use their strategies with highest scores. A strategy in a given time is considered successful if it correctly predicts the minority side. The strategies with highest scores are those which were the most successful in the previous turns of the game.

Some papers have addressed the question of how to incorporate the concept of intelligence in the MG [43,44]. One interesting characteristic of this game is that even when non-intelligent agents are playing the game, these agents are organized around the optimal setup of the game [45]. However, it was shown for the standard MG that, when intelligent agents are playing the game, the fluctuations around the optimal value may be reduced [7].

In the MG version with local information exchange, some of the playing agents believe that their neighbors may be better informed than themselves. A wealthier (or better informed) agent B, with respect to agent A, has been more successful in predicting the minority side in the previous game turns than A. When some agents are ready to blindly follow their wealthiest neighbors, a new type of collective phenomenon, called herding behavior, may emerge. Economic theory, which is said to have been built basically based on deductive reasoning, asserts that such decision is rational, even when the agent's former information, suggesting a different decision, is ignored [46]. Actually, one should notice that if not only one, but many agents follow the best informed agent of their neighborhoods, the best informed agent will soon be in the majority side, and he will no longer be followed.

To implement the information exchange, at each game turn every agent looks for the wealthiest agent located in his neighborhood. Considering that every agent starts the game with the same endowments, the wealthiest agent here is the one that has achieved the larger number of successes in the previous turns of the game. Then, each agent compares his own wealth with the wealth of this wealthiest agent in his neighborhood. If this wealthiest agent is wealthier than him, he follows his wealthiest neighbor. Otherwise, he follows his own strategy.

3 A MG based network evolution model

In opposition to the local information exchange model [19], where the neighborhood structure was set up

by an ad-hoc complex network, we consider herein that networks are dynamically built by taking into account MG outcomes. Such MG-networks evolve in time according to a three parameter model, which is defined as follows. First assign to any network node i a variable called wealth $0 \leq w_i \leq 1$. w_i is the normalized count of the number of successes that agent i has experienced in choosing the minority side in the previous game turns. The MG starts at time $t = -\eta$, when $w_i = 0, \forall i$, and all agents are decoupled from each other. Then we compute the value of w_i in the $[-\eta, 0]$ interval, where η indicates a time lag necessary to obtain a typical wealth distribution before the agents start to build the network at $t = 0$.

From this time on, we assume that, at each time step, the probability that two unconnected nodes i and j become connected is proportional to

$$\frac{\kappa_c}{N-1}\, e^{-\beta|w_i - w_j|}, \tag{1}$$

where the inverse temperature parameter β gauges the relative weight of the wealth proximity and κ_c controls the overall connection probability. On the other hand, an existing connection may be broken with probability $\kappa_d < 1$. These rules are based on the basic ideas of preferential social distance attachment.

In this model, one time step corresponds to selecting $\kappa_d N(N-1)/2$ pairs of nodes, and updating their status, i.e.: (i) disconnect the selected nodes in the case the selected nodes are connected; (ii) in the case they are not connected, a connection between the nodes is created with probability $p_{ij} = \frac{\kappa_c}{\kappa_d(N-1)} e^{-\beta|w_i - w_j|} = e^{-\beta \Delta E_{ij}}$, with

$$\Delta E_{ij} = |w_i - w_j| - \frac{1}{\beta} \ln \frac{\kappa_c}{\kappa_d (N-1)}. \tag{2}$$

If $\kappa_c/(N-1) < \kappa_d$, this dynamics is equivalent to the one described by the Metropolis algorithm, where the energy of the connected state is larger than the energy of the unconnected state by ΔE_{ij}.

The above described simulation scheme becomes very inefficient whenever the number of links $N_E \ll N(N-1)/2$ and $\frac{\kappa_c}{\kappa_d(N-1)} \ll 1$. In that case, it is better to randomly choose $\kappa_d N_E$ links to be broken at each time step. Simultaneously, $\frac{\kappa_c(N(N-1)/2 - N_E)}{\kappa_d(N-1)}$ pairs of unconnected nodes should be selected and connected with probability $e^{-\beta|w_i - w_j|}$.

The time evolving MG-network eventually reaches a stationary state if the wealth distributions also does the same, what is evident when global variables are plotted against time, as shown latter in this paper. Neither the richness nor the network become static when the stationary state is reached. Nevertheless, it is useful to understand what would happen if the network evolved among player with fixed richness. In such case, the connection probability between two nodes is obtained by equating the flow in both directions, i.e.,

$$(1 - p_{ij})\, \frac{\kappa_c}{N-1}\, e^{-\beta|w_i - w_j|} = p_{ij} \kappa_d, \tag{3}$$

where p_{ij} is the probability that nodes i and j are connected. From equation (3) we can immediately obtain the steady state values

$$\begin{aligned} p_{ij} &= \frac{1}{1 + \frac{\kappa_d}{\kappa_c}(N-1)\, e^{\beta|w_i - w_j|}} \\ &\approx \frac{\kappa_c}{\kappa_d (N-1)}\, e^{-\beta|w_i - w_j|}. \end{aligned} \tag{4}$$

The above approximation is valid for $(N-1) \gg \kappa_c/\kappa_d$.

The interpretation of equation (2) is that it takes more energy to establish a connection in a bigger population. However, if κ_c, κ_d and β are the same, whatever the size of the population, their members will have, in average, the same number of neighbors. Indeed, the increase in the energy is compensated by a larger number of accessible people. The chances are that an agent is linked to a significative fraction of his neighbors within a social distance

$$|w_i - w_j| < \frac{1}{\beta} \ln \frac{\kappa_c}{\kappa_d (N-1)}. \tag{5}$$

Beyond this threshold value, it is increasingly less probable that the agents know each other the larger the value of $|w_i - w_j|$.

It is important to make clear that the main rates behind the dynamics of the two components of the model are the rate of network formation and the rate of agents learning.

As shown above, the structure of a network evolving with a frozen wealth distribution is controlled by the parameter β and by the ratio κ_c/κ_d. Simultaneously multiplying κ_c and κ_d by the same value, does not affect the resulting structure, but rescale the time.

The learning rate of the MG agents is proportional to 2^{-M}. It is interesting to have an alternative formulation of the network dynamics where that rate is included. In this formulation, the parameters κ_c and κ_d are replaced by the parameters κ and R. κ controls the overall network evolution rate and R controls the connecting and disconnecting bias. These parameters are related y

$$\kappa = \frac{\kappa_c + \kappa_d}{2^M}, \tag{6}$$

$$R = \frac{\kappa_c}{\kappa_d}, \tag{7}$$

$$\kappa_c = \kappa \frac{R}{1+R} 2^M, \tag{8}$$

$$\kappa_d = \kappa \frac{1}{1+R} 2^M. \tag{9}$$

It is important to notice that the effect of M in the dynamics goes beyond the proportionality of the learning rate to 2^M. Due to the dependence of the network formation on w and β, the network evolution rate depends not only on κ. Because of that, it is not possible to write a comprehensive formulation regarding only the effect of M in the network evolution rate.

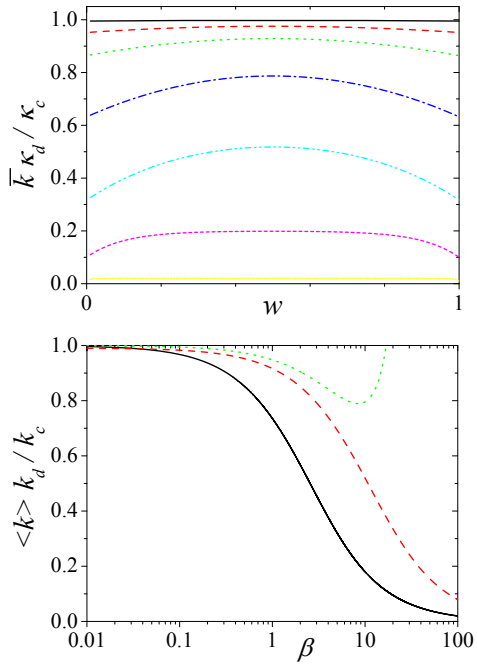

Fig. 1. (Color online) (a) Graphical illustration of equations (11), (12), and (14). (a) $\bar{k}(w)$ as function of w, for $\rho(w) = 1$, and several values of β (from top to down, $\beta = 0.01, 0.1, 0.3, 1, 3, 10, 100$). (b) $\langle k\rangle$ as function of β, for $\rho(w) = 1$ (black solid line) and $\rho(w) = \sqrt{\gamma/\pi}\exp[-\gamma(w - w_0)^2]$ (red dashes). This curve was obtained after the numerical integration of equations (10) and (12). Green dots correspond to the approximation of this integral provided by equation (14). For both curves, we consider $\gamma = 100$ and $\omega_0 = 0.8$.

3.1 Analytical estimates

As we will discuss in the next section, important features of MG-networks strongly depends on the particular wealth distribution $\rho(w)$. Although such distribution results from MG outputs, it is possible to derive some analytical results under the assumption that the two-node wealth distribution function $\rho_2(w, w') \approx \rho(w)\rho(w')$, and that $\rho(w)$ satisfies some particularly symmetric conditions. For instance, let us consider that the average degree of a particular agent with wealth w can be expressed in terms of the normalized distribution of nodes $\rho(w)$ and equation (4) by

$$\bar{k}(w) \approx \frac{\kappa_c}{\kappa_d}\int \rho\,(w')\; e^{-\beta|w-w'|}\,dw'. \qquad (10)$$

If we assume a uniform distribution of $\rho(w)$ in the $[0, 1]$ interval, the above expression can be easily evaluated as

$$\bar{k}(w) \approx \frac{\kappa_c}{\beta\kappa_d}\left(2 - e^{-\beta w} - e^{-\beta(1-w)}\right). \qquad (11)$$

The average value $\langle k\rangle$ taken over the whole w interval follows immediately as

$$\langle k\rangle = \int_0^1 \bar{k}(w)\rho(w)dw \approx \frac{2\kappa_c}{\beta^2\kappa_d}\left(\beta + e^{-\beta} - 1\right), \qquad (12)$$

as illustrated in Figures 1a and 1b.

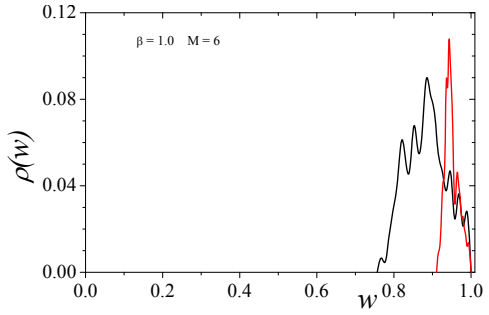

Fig. 2. (Color online) Asymptotic form of the wealth distribution $\rho(w)$ for $\beta = 1.0$, $M = 6$, $N = 101$ (black solid line) and 317 (red dashes).

Using the further assumption that the agents are placed on a linear chain according to their wealth, it is also possible to derive the density ϱ of the normalized spatial length $0 \le W \le 1$ between the connected nodes as

$$\varrho(W) = \frac{N(N-1)}{1 + \frac{\kappa_d}{\kappa_c}(N-1)e^{\beta W}}\int \rho(w)\rho(w+W)dw$$
$$\approx \frac{\kappa_c}{\kappa_d}N\,e^{-\beta W}\int \rho(w)\rho(w+W)dw. \qquad (13)$$

For the previously used uniform distribution of wealths, the integral in equation (13) reduces to $1 - W$.

On the other hand, if we assume that the wealth is distributed by a gaussian function, $\rho(w) \sim \exp[-\gamma(w - w_0)^2$, it is possible to obtain an approximate result

$$\langle k\rangle \approx \frac{\kappa_c}{\kappa_d}\exp\left(\beta^2/2\gamma\right)\left[1 - \mathrm{erf}\left(\frac{\beta}{2\sqrt{\gamma}}\right)\right], \qquad (14)$$

which is valid under the restriction that $\beta/2\sqrt{\gamma} \ll 1$.

From equation (14) we note that, in the limit of a Dirac's $\delta(w - w_0)$ distribution, we obtain $\langle k\rangle = \frac{\kappa_c}{\kappa_d}$. For a fixed finite value of γ, $\langle k\rangle$ also decreases with β within the region where $\beta/2\sqrt{\gamma} \ll 1$, as shown in Figure 1.

4 MG-network properties

4.1 MG-networks

In this section we explore how the network evolves when the agents do not communicate with each other when deciding how to play. The numerical simulations allow for the evaluation of a rich set of measures that characterize the network and MG outputs. The process of network construction initially goes through a transient phase, which is followed by a relaxation towards an asymptotic stationary configuration. Such configuration is not static, since edges between nodes are continuously added and removed from the network at each game turn, but the network measures attain constant values.

In Figure 2 we show that the asymptotic wealth distribution among the agents resulting from the numerical simulations is not widely distributed over the $[0, 1]$ interval, but concentrated within a small region of width $\simeq 0.2$

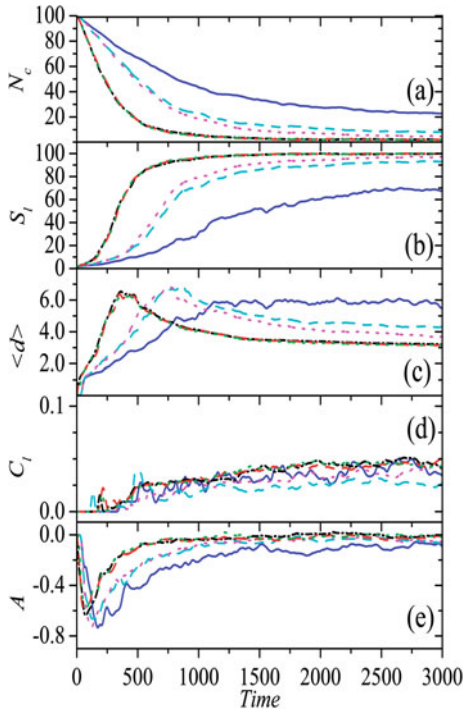

Fig. 3. (Color online) Time evolution of the several network measures (Number of clusters N_c (a), size of the largest cluster S_l (b), average shortest path in the largest cluster $\langle d\rangle_l$ (c), clustering coefficient of the largest cluster C_l (d), and assortative coefficient of the largest cluster A_l (e)), resulting from the dynamic network wiring according to the rules discussed in Section 3. Black solid line, red dashes and green dots indicate, respectively, results for networks obtained when the number of memories $M = 2, 6$, and 10. In the plots above shown, these three memories collapse in one curve. Parameter values are $N = 101$, $\kappa_c = 0.005$, $\kappa_d = 0.001$, and $\beta = 0.1$. Curves for $\beta = 10$ and same values of κ_c and κ_d are drawn with blue solid lines, cyan dashes and magenta dots, respectively for $M = 2, 6$, and 10.

what justifies the choice of the values of γ and ω_0 in Figure 1b. The general aspects of the dependence of node degree with respect to the model parameters indicate that, in general, $\langle k\rangle$ decreases with β. This behavior sets limits to the validity of the results in the previous section, since the approximation used when deriving equation (14) is only valid when $\beta \ll 2\sqrt{\gamma}$.

In Figure 3, five panels present two typical time evolution patterns for the following measures: (a) the number of isolated clusters N_c; (b) the size S_l of the largest cluster Cl_l; (c) the average shortest path $\langle d\rangle_l$ in Cl_l; (d) the clustering coefficient C_l in Cl_l; (e) the assortativity coefficient A_l in Cl_l.

We consider $N = 101$, $\kappa_c = 0.005$, $\kappa_d = 0.001$, and draw two groups (for $\beta = 0.1, 10$) of three curves corresponding to $M = 2, 6$, and 12. A small value of N was chosen as it allows for a clearer display of several of the main features of the network evolution. Our results have been systematically collected for larger values $N = 317$, 1001, and 3171.

At $t = 0$, the system consists of N isolated nodes. As time increases, the model rules introduce links between pairs of nodes so that, as expected, N_c decreases and S_l increases. Figures 3a and 3b illustrate the monotonic decrease of N_c and sigmoidal shape of S_l indicating that, as $t \to \infty$, almost all nodes belong to the largest cluster. The observed fluctuations in $S_l \sim N$ results from dynamical removal and insertion of connections. The dominant effect of increasing β is to increase both the required time for building up the largest cluster and the fluctuations in the value of S_l. A similar effect is played by the ratio $R \equiv \kappa_c/\kappa_d$, as long as $R > 1$. As long as β is small, the overall effect of M in the network evolution is negligible but, for larger values (e.g. $\beta = 10$), we notice that N_c and S_l evolves more rapidly to their limiting values when $M \geq 3$. An overall reduction on the value of of S_l is observed in the neighborhood of the threshold value $R = 1$ (not shown). If $R < 1$, it is difficult to the network to preserve its structure due to the large removal of connections, so that $N_c \sim N$ and $S_l/N \ll 1$. The value of R is directly related to the network average degree $\langle k\rangle = \sum_i k_i/N$, where k_i is the degree (number of neighbors) of node i.

The time evolution of $\langle d\rangle_l$ is characterized by the presence of a maximum, located at roughly the same value of t at which $N_c \simeq N/3 \simeq S_l/2$. This feature is independent of the variation of β, whenever the condition $R > 1$ is valid. Therefore, a faster increase in S_l causes the maximum in $\langle d\rangle_l$ to occur at smaller values of t. Finally, an increase in the value of β and/or R favors the increase of the $t \to \infty$ value of $\langle d\rangle_l$. We observed that such influence firstly ($\beta \sim 10$) affects the curves with low values of M only. Of course $\langle d\rangle_l$ depends on the number of agents N. In Figure 4a, we show the behavior of $\langle d\rangle_l$ as function of N for five different sets of parameter values. The results indicate that $\langle d\rangle_l \sim \log N$.

We notice that the clustering coefficient C_l in Figure 3d remains very small for all values of t, although when $\beta = 0.1$ larger values than when $\beta = 10$ are obtained. This indicates that, for the used values of the model parameters, the formation of cliques is rather small. Since equations (2) and (12) indicate that $\langle k\rangle$ is directly proportional to R, larger values of C_l can only be expected when R is much larger than the value used in Figure 3. In such situation, larger values of C_l first appear when $M = 2$ but, by further increasing the value of R, C_l becomes roughly independent of M. Finally, the dependence of C_l on N, for fixed values of parameters β, κ_c, and κ_d, is shown in Figure 4b. Such decreasing behavior is typical for non-structured networks with fixed average number of neighbors.

The overall behavior of A_l indicates dissortative properties which are quite evident during transient time. Its time evolution is characterized by a rapid decrease to a negative value, much earlier than that one observed for $\langle d\rangle_l$. This is followed by a relaxation to the negative region close to $A_l = 0$. Since the minimum occurs at very small values of $N_c/N \sim 0.1$, it seems that this peak is devoid of a useful meaning to characterize the network structure. The position of this peak in the time axis is subject to

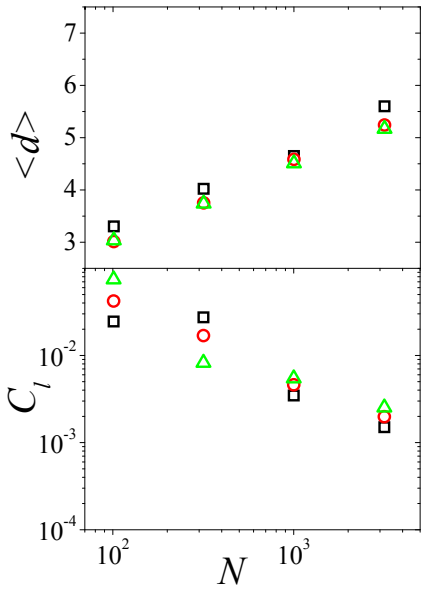

Fig. 4. (Color online) Dependence of $\langle d\rangle_l$ (a) and C_l (b) on the number of agents N after the network reaches the stationary regime ($t > 1000$), for the same parameter values as in Figure 3. Networks for $M = 2, 6$ and 10 are indicated by black squares, red circles and green triangles. Panel (a) indicates that $\langle d\rangle_l \sim \log N \sim \log N_l$. Panel (b) indicates that C_l decreases with N for fixed average number of node degree κ_c/κ_d.

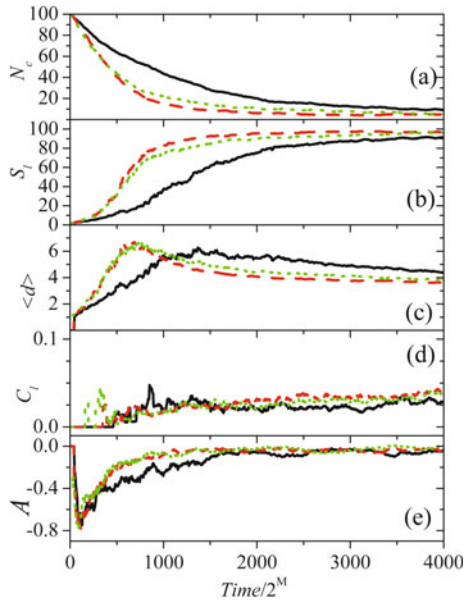

Fig. 5. (Color online) Effect on the network formation due to the explicit M dependence of κ_c and κ_d introduced in equations (6) to (9), for the same measures displayed in Figure 3 with $\beta = 10$. Time was rescaled to show the partial collapse of the time series due to the 2^M learning rate. For $\beta = 0.1$ the curves do not collapse any more like in Figure 3, but spread out due their own time scales as for beta = 10. Values of M closer to each other were selected: 2 (black), 4 (red) and 6 (green). The curves clearly reflect the explicit dependence on M introduced on the rate constants to describe the effect of the MG learning scale. This can be easily seen, for instance, in the shifted maxima of $\langle d\rangle$. Such simple effect can not be easily repeated just by tuning the values of β.

the same influence of the parameter values for the already discussed features. As $t \to \infty$, the overall tendency is to weaken the dissortative character as $A_l \to 0$.

As shown in Figure 3, the network evolution depends on M through the selected values of κ_c, κ_d and β. The curves indicate, however, that only for the larger value $\beta = 10$ there is a noticeable dependence on M. This is certainly related to the functional form assumed for the proposed model. In order to turn explicit influence of M in the network formation, it is necessary to use the generalization for the definition of κ_c and κ_d expressed by equations (6) to (9). In such case, the typical time required for the network formation depends on M according to the explicit form indicated in equations (6) to (9). This can be made clearer by the time of occurrence of the maximum of $\langle d\rangle$, as shown in Figure 5. We emphasize that these results, together with those in Figure 3 turn it clear that the implicit dependence of β on the time formation for different M is not simple, and can not easily be inferred as in the case of κ_c and κ_d.

4.2 Feedback MG-networks

The networks discussed sofar evolve in time while MG is played, but they do not influence the game outputs, as each agent considers only the strategies of its own memory book. The effect of a feedback mechanism, in which the agents can decide to take into account the strategies of their neighbors in the network, will be discussed in the next section. However, it is important to notice that such changes in the agents decision can cause further influence on the network themselves. In this sub-section we investigate to which extent the feedback MG-networks (FMG-networks) are distinct from those discussed before.

Here, as well as in the next section, we consider three different algorithms ($A1 - A3$) to take into account the reciprocal influence of the neighbor's strategies on each agent decision. Two of them ($A1, A2$) have already been introduced in [19]. The third one ($A3$), which we introduce here, is in some sense an interpolation between the two former algorithms. In $A1$ we suppose that the agent i, who considers the possibility of imitating his neighbors, has access only to the highest scored strategy of the wealthiest neighbor, but not to his wealthiest neighbor's current time action. Such dynamics, in which all agents play at the same time, can be thought as being similar to a parallel update in cellular automata (CA) models. Note that in this situation, the agent's decision may be different of the decision of his wealthiest neighbor who may not follow his own strategy if he imitates his own wealthiest neighbor.

The second algorithm $A2$ supposes that the agent has complete access to the current decision of his wealthiest neighbor. In this later case, if the given wealthiest neighbor of the agent is already following another neighbor, then, even in this case, the agent will copy the action of

his wealthiest neighbor. In fact, behind this idea, it is being supposed that the least wealthy agents wait until the wealthiest neighbors play the game.

The third choice, $A3$, amounts to consider that the agents play in a random order. At his playing turn, agent i will also imitate the decision of his wealthiest neighbor, but he is not aware if he will have access to the highest scored strategy or to the last action of the wealthiest neighbor. This depends on whether his wealthiest neighbor has or has not played before him. $A2$ is a special $A3$ sequential update, in which the wealthiest agents play first.

The obtained results for networks generated with the inclusion of feedback mechanisms indicate that, independently of the chosen strategies $A1 - A3$, the changes in the five measures displayed are rather small for all values of β and $R > 1$. From a qualitative point of view, no significative difference between Figure 3 and its corresponding version for the altered evolution. Quantitative changes refer to a small decrease (increase) in the asymptotic value of $\langle d \rangle_l (C_l)$. Another minor change observed in the network dynamics refers to a slight increase in the pace at which the asymptotic values of all five measures shown in Figure 3 when algorithms $A1 - A3$ are turned on.

4.3 ER-networks and other measures

In order to obtain a clearer picture of the structures present in the MG- and FMG-networks, we evaluated some more detailed measures after freezing the network evolution at some large values of time (typically $t = 10^3$, 3×10^3, and 10^4). For the purpose of comparison, we generated random Erdös-Renyi (ER) networks with the same number of nodes and constant probability attachment p that leads to the same average degree $\langle k \rangle_l$ as the MG/FMG-networks.

In Figures 6a and 6b we show the degree probability distribution function $P(k)$ (PDF) for, respectively, the MG/FMG networks generated with MG memory of size $M = 2$ at freezing time $t = 500$, and their corresponding ER counterparts. We use the same values of κ_c and κ_d as in Figure 3, but $\beta = 3$ and $N = 1001$. For the used freezing time and parameter values, the evolved network has already reached the asymptotic region. The comparison of the curves in the two panels indicate that the distributions agree quite well for all four networks. This result, together with that one obtained for the clustering coefficient C_l, implies that MG dynamics does not lead to networks that fit into the typical scale-free and small-world scenarios. Rather, they hint that the asymptotic network shares the ER properties. In Figures 6c and 6d we illustrate the $P(k)$'s for the $M = 6$ and 10 MG/FMG networks. The main difference with respect to the distributions shown in Figure 6a is observed in the position of the $P(k)$ for the MG-network. For both values of M, it has been displaced to the right, so that it superposes with the other three $P(k)$'s obtained for the $A1 - A3$ FMG-networks. For $M = 10$, the differences between the four distributions have been reduced to a minimum, indicating that the influence of the feedback algorithms is almost negligible in the network evolution. As for $M = 2$, the curves in Figures 6c and 6d agree quite well with the corresponding PDF's for the ER networks (not shown). Finally, the fact that all distributions are peaked in the neighborhood of $k = 5$ can be explained by the by the fact $\kappa_c/\kappa_d = 5 \approx \langle k \rangle$ for all four panels of Figure 5.

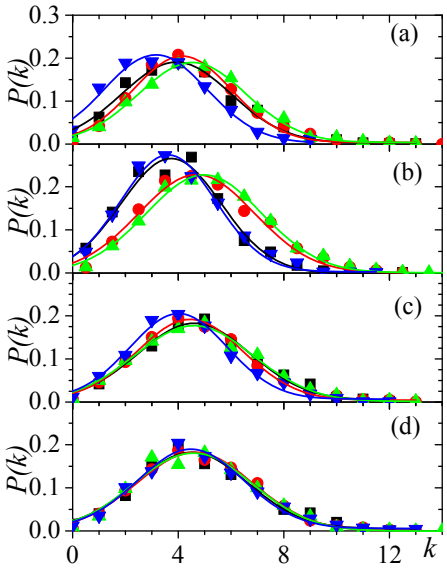

Fig. 6. (Color online) Degree distribution for MG- and FMG-networks. Black squares, red dots, and green up triangles indicate results for $A1 - A3$ feedback algorithms, while blue down triangles corresponds to standard MG-network. Solid lines were obtained by gaussian fits to scattered points. Parameter values are $N = 1001$, $\kappa_c = 0.005$, $\kappa_d = 0.001$, and $\beta = 3.0$. In (a) we consider $M = 2$ and in (b) the results are for ER equivalent networks to those in (a). (c) and (d) correspond to $M = 6$ and $M = 10$, respectively.

The same indication is supported by the comparison of the clustering coefficients C for the MG and ER networks. For all values of β, the value of C for corresponding ER network is of the same order of magnitude as C_l indicated in Figure 3d.

We have also characterized the network structure by looking for signatures of fractal features (in the sense discussed in [47]), as well as for the presence of well defined communities. In this latter case, we applied the Newman-Girvan algorithm, based on the successive elimination of links with highest degree of betweenness, in order to detect the presence of modular properties. Although we explored a large range of values of β and several values of the memory M, no such structural arrangement could be detected.

Fractal properties, expressed by power law dependence between the minimal number of clusters $N_c(d)$ encompassing nodes that are at most d steps apart and the actual value of d, can only be assigned to those networks that have large values of diameter D. In the current model, this restricts the possible occurrence of such properties to small values of both κ_c and β. In despite of a search in the region of small values of β, we have no succeeded

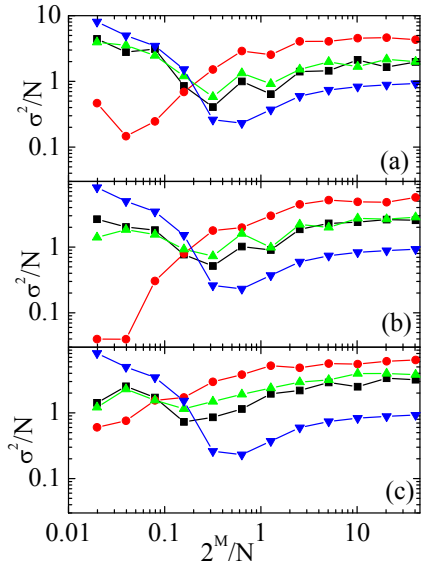

Fig. 7. (Color online) Dependence of σ^2/N on α for $N = 101$, $\kappa_c = 0.005$, $\kappa_d = 0.001$, and $\beta = 3$. Results are rather insensitive to the value of N. Black squares, red dots and green up triangles indicate results for algorithms $A1 - A3$, while blue down triangles correspond to standard MG result. Freezing network time are $\tau = 1000(a), 3000(b)$, and $10000(c)$. A decrease of σ below the absolute minimum of standard MG was not found for a priori introduced networks [19].

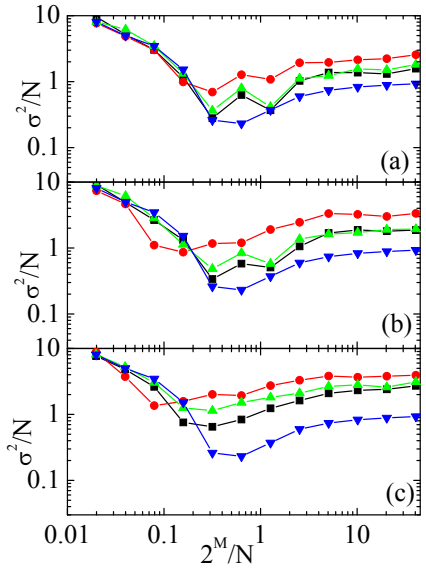

Fig. 8. (Color online) Dependence of σ^2/N on α for $\beta = 30$. Other parameter values are the same as in Figure 7. The results for $M \leq 4$ are much closer to the standard MG than those for $\beta = 3$. As before, results are always worse than standard MG for $M \geq 5$.

in finding convincing evidences that any of the obtained networks displays fractal property.

To close this section, we remark that a general feature of the networks obtained by the model is the absence of communities characterized by the richness degree, in opposition to other social networks with such feature [35,36,48–50]. A small number of exceptions to this framework refers to networks obtained for extremely larger values of R and small values of M.

The same indication of absence of communities has been given by an initially negative assortativity coefficient which, with the time evolution, reduces it absolute value, indicating a weak dissortative character in the asymptotic regime.

Despite the fact that the obtained networks do not share some of the expected properties of social networks, the interaction between agents do affect the results of the MG outcomes, as will be discussed in the next section.

5 Influence of network structure on MG outputs

The influence of the network structure on MG outputs is summarized in the plots displaying the dependence of the normalized volatility σ^2/N on $\alpha = 2^M/N$, the normalized number of accessed memories. For such situations, it is clear that the feedback effect on the network evolution must be taken into account. Because the network evolves with time, we have also taken into account the effect of the network freezing time τ. Results for small and large values of β are drawn in Figures 7 and 8, which show the dependence of σ^2/N at three different values of τ. For the sake of a better comparison, we also draw the dependence for the classical independent agents MG version.

For $\beta = 3.0$, our results show that σ^2/N is greatly reduced by the network structure when $M \leq 4$. The algorithm $A2$ is the most effective in reducing σ. For $M = 2$ and $M = 3$, absolute minima even lower than the value 0.264 observed at $M = 6$ in the conventional MG are attained. This scenario is consistently observed for $\tau = 1000$ and 3000 (see Figs. 7a and 7b). This contrasts with previous results induced by the fixed network structure [19], where no more efficient result for σ had been reported. Algorithms $A1$ and $A3$ also cause a reduction in the volatility within the same interval $M \leq 4$, but the new values are larger than the conventional MG minimum. For $\tau = 10000$, Figure 7c shows that σ increases with respect to the behavior at previous values of τ and approaches the results from standard MG for low values of M.

For $M \geq 5$, the herding behavior induced by any of the three algorithms reduces the MG output efficiency. Values of σ have increased with respect to corresponding conventional MG results, the worse result being provided by algorithm $A2$. In this range of value of M, the volatility largely surpasses the results from random decision making. We recall that the usual interpretation of conventional MG reaching this limiting value in the limit of large M is that the agents are not able to extract useful information from common memory.

For $\beta = 30$, the results in Figure 8 indicate that the interaction between neighboring agents strongly reduces its influence in lowering the value of σ for small values of M. For larger values of M, the behavior is roughly the same, lying above the result for the standard MG. It

is important to refer to Figure 1, that shows the overall tendency of low values of "temperature" is to reduce the number of neighbors in the network. Thus, independently of the used algorithm, the three curves in Figure 8 hint that at larger values of β the tendency of the curves is to overscore that of the standard MG.

Once the overall influence of β can be understood, the most striking difference is the strong reduction in σ for low values of M (≤ 4) for the networks that evolve with low values of β, as those for $\beta = 3$ shown in Figure 7. This can be understood by recalling that the small number of strategies that are present for such cases implies that, without herding behavior the ability of an agent for playing the game is strongly dependent on the chance of getting in the beginning of the game a good strategy book. Furthermore, the structure of a network built with small values of β allows with considerable probability, the existence of links between wealthy (the ones that have the best strategies) and poor agents (the ones that have the worse strategies). Therefore, algorithm A2 together with the likely presence of links between wealthy and poor agents improves the way that the available information is used. For the cases of algorithms A1 and A3, one can note that this effect is weaker due the less efficient flow of information present in these algorithms. Finally, this phenomenon does not happen for high values of M (≥ 5), since in these situations there is a much larger number of strategies and the presence of herding behavior in this case is a source for increasing the correlation among the strategies generating higher volatility.

6 Conclusion

In this paper, we have considered the interaction between MG agents with local information, where the agents herd their neighbors if their neighbors are wealthier them themselves. Interaction mediates the construction of a network that evolves over time, based on the social distance measured by the wealth of the agents that are playing the game. In order to characterize this system we have presented analytical results and also simulation-based results.

We presented a characterization of the emerging network properties as well as their influence on MG outputs. Despite the fact that links are preferentially created between nodes with similar wealth, the resulting networks show no clear evidence of a large scale structure, as a scale-free distribution of node degree, modularity or large clustering coefficient. Larger values of C_l can be obtained but only if κ_c largely exceeds κ_d, but this leads to a very larger value of $\langle k \rangle$, what drives the resulting structure out of the common pattern of the complex network.

The results for MG outputs show that dynamically created networks may indeed lead to better game performances. This proves that, even if the networks seem unstructured, they are not equivalent to pure random ER networks. Indeed, for such situation, the previous results [19] have shown that the game performance is worse than conventional MG. The effect of both temperature and memory size seems to be crucial for the improvement of the MG performance, although their influence are exercised in different ways: temperature impacts network formation, while memory size impacts the ability of the system to extract useful information.

Such dependence can also be analyzed from the point of view of the interplay between the time scale imposed by network evolution and the one resulting from MG itself. If the above discussion follows the large majority of published works, treating the influence of M on the outputs from the point of view of the ability of the agents to deal with information provided the last outcomes, we may also interpret the role of M defining a proper time scale for the game. Therefore, it happens that for some values of model parameters, as $\beta = 0.1$ in Figure 3, the influence of M is minor, as the network evolution time scale is much shorter than that of MG. On the other hand, the same figure shows that, for larger values of β, this time scale increases, so that the whole system is able to take into account also the influence of the time scale imposed by M.

These observations are corroborated by the results presented in the Section 5. There we have shown that the dependence of the volatility on M also depends both on β as well as on M, indicating that the interplay of both time scales influence the results of the proposed model.

We think the proposed framework can be further explored in different directions. The most obvious one being the finer scanning of the parameter space. Particularly, the interplay between R and β might identify networks with more clear structure and smaller values of $\langle k \rangle$. Other features to be investigated include intermittent updates in network evolution and their influence in the wealthy distribution among MG agents.

The authors thank the Brazilian Agency CNPQ for financial support.

References

1. B. LeBaron, J. Econ. Dyn. Control **24**, 679 (2000)
2. N.F. Johnson, P. Jefferies, P.M. Hui, *Financial market complexity* (Oxford University Press, Oxford, 2003)
3. D. Challet, Y.C. Zhang, Physica A **246**, 407 (1997)
4. W.B. Arthur, Am. Econ. Rev. **84**, 406 (1994)
5. A.C.C. Coolen, *The mathematical theory of minority games* (Oxford University Press, Oxford, 2005)
6. D. Challet, M. Marsili, Y.C. Zhang, *Minority games* (Oxford University Press, Oxford, 2005)
7. R. Savit, R. Manuca, R. Riolo, Phys. Rev. Lett. **82**, 2203 (1999)
8. T. Kalinowski, H.-J. Schulz, M. Briese, Physica A **277**, 502 (2000)
9. S. Moelbert, P.D.L. Rios, Physica A **303**, 217 (2002)
10. A. Galstyan, K. Lerman, Phys. Rev. E **66**, 015103 (2002)
11. H.J. Quan, B.H. Wang, P.M. Hui et al., Physica A **321**, 300 (2003)
12. H.F. Chau, F.K. Chow, K.H. Ho, Physica A **332**, 483 (2004)

13. Y. Li, R. Savit, Physica A **335**, 217 (2004)
14. E. Burgos, H. Ceva, R.P.J. Perazzo, Physica A **337**, 635 (2004)
15. I. Caridi, H. Ceva, Physica A **339**, 574 (2004)
16. L. Shang, X.F. Wang, Physica A **361**, 643 (2006)
17. M. Kirley, Physica A **365**, 521 (2005)
18. H. Lavicka, F. Slanina, Eur. Phys. J. B **56**, 53 (2007)
19. D.O. Cajueiro, R.S. DeCamargo, Phys. Lett. A **355**, 280 (2006)
20. D.O. Cajueiro, Phys. Rev. E **72**, 047104 (2005)
21. M.O. Jackson, B.W. Rogers, J. Eur. Econ. Assoc. **3**, 617 (2005)
22. R. Carvalho, G. Iori, Phys. Rev. E **78**, 016110 (2008)
23. P. Erdós, A. Rényi, Bulletin of the International Statistical Institute **38**, 343 (1960)
24. D.J. Watts, S.H. Strogatz, Nature **393**, 440 (1998)
25. D.J. Watts, *Small worlds: the dynamics of networks between order and randomness* (Princeton University Press, Princeton, 1999)
26. A.L. Barabasi, R. Albert, Science **286**, 509 (1999)
27. C. Castellano, S. Fortunato, V. Loreto, Rev. Mod. Phys. **81**, 591 (2009)
28. M.L. Lyra, U.M.S. Costa, R.N.C. Filho et al., Europhys. Lett. **62**, 131 (2003)
29. A.A. Moreira, D.R. Paula, R.N. Costa et al., Phys. Rev. E **73**, 065101 (2006)
30. P.G. Lind, L.R.D. Silva, J.S.A. Jr. et al., Phys. Rev. E **76**, 036117 (2007)
31. A.A. Moreira, A. Mathur, D. Diermeier et al., Proceedings of the National Academy of Sciences of the United States of America **101**, 12085 (2004)
32. B.A. Mello, L.H. Batistuta, R. Boueri et al., Phys. Lett. A **28**, 126 (2009)
33. V. Schwammle, M.C. Gonzalez, A.A. Moreira et al., Phys. Rev. E **75**, 066108 (2007)
34. M. Anghel, Z. Toroczkai, K.E. Bassler et al., Phys. Rev. Lett. **92**, 058701 (2004)
35. M. Boguña, R. Pastor-Satorras, A. Diaz-Guilera et al., Phys. Rev. E **70**, 056122 (2004)
36. G.C.M.A. Ehrhardt, M. Marsili, F. Vega-Redondo, Phys. Rev. E **74**, 036106 (2006)
37. A. Grabowski, R.A. Kosinki, Phys. Rev. E **73**, 016135 (2006)
38. E.M. Jin, M. Girvan, M.E.J. Newman, Phys. Rev. E **64**, 046132 (2001)
39. D.J.B. Soares, C. Tsallis, A.M. Mariz et al., Europhys. Lett. **70**, 70 (2005)
40. L.H. Wong, P. Pattison, G. Robins, Physica A **360**, 99 (2006)
41. K. Kosmidis, S. Havlin, A. Bunde, Europhys. Lett. **82**, 48005 (2008)
42. R. Lambiotte, V.D. Blondel, C. De-Kerchove et al., Physica A **387**, 5317 (2008)
43. J. Wakeling, P. Bak, Phys. Rev. E **64**, 051920 (2001)
44. B.A. Mello, D.O. Cajueiro, Physica A **387**, 557 (2008)
45. D. Challet, M. Marsili, G. Ottino, Physica A **332**, 469 (2004)
46. C.P. Chamley, *Rational herds: economic models of social learning* (Cambridge University Press, Cambridge, 2004)
47. C. Song, S. Havlin, H.A. Makse, Nature **433**, 392 (2005)
48. M.E.J. Newman, Phys. Rev. Lett. **89**, 208701 (2002)
49. M.E.J. Newman, J. Park, Phys. Rev. E **68**, 036122 (2003)
50. R. Toivonen, J.P. Onella, J. Saramaki, Physica A **371**, 851 (2006)